



Cite this: *J. Anal. At. Spectrom.*, 2025,  
40, 1098

## Lithium isotope analysis on the Neoma MS/MS MC-ICP-MS

Sean R Scott, \* Gabrielle L Turner, Brandy N Gartman, Sonia Alcantar Anguiano, Kali M Melby, Barbara E Allen, Travis D Minton, Matthew A RisenHuber and Kirby P Hobbs

Lithium isotopes are measured routinely using multi-collector inductively coupled plasma mass spectrometry due to the high throughput and high measurement precision capabilities of this technique. To obtain high precision isotopic data, lithium is generally purified through ion exchange resins to reduce compositional matrix effects and minimize isobaric interferences when analyzed in solution. In this work, we demonstrate that the ThermoScientific Neoma MS/MS MC-ICP-MS can be used to measure high precision lithium isotopic ratios after purification for a variety of geological and environmental matrices. While the double-Wien filter of the Neoma MS/MS requires additional considerations for measuring lithium isotopes compared to previous generation instruments, high precision lithium isotope ratios can be achieved with proper tuning of the lenses. We provide a strategy for optimization of  ${}^6\text{Li}/{}^7\text{Li}$  measurements for precision and measurement stability, and show our long-term reproducibility for NIST924a and IRMM-016 was 0.8‰ and 0.5‰, respectively. In addition, we provide new  ${}^6\text{Li}/{}^7\text{Li}$  measurements for several environmental reference materials without Li isotope data in the literature, including NIST SRMs 1646a, 2706, 2711a, 2780a, and 4350b.

Received 22nd November 2024  
Accepted 4th March 2025

DOI: 10.1039/d4ja00419a

rsc.li/jaas

### 1. Introduction

The need for lithium isotopic analysis has expanded across many scientific disciplines, including applications in a variety of earth science fields,<sup>1–7</sup> as well as forensic<sup>8</sup> and nuclear<sup>9–11</sup> research. Analytical methods vary widely, with the use of thermal ionization mass spectrometry (TIMS;<sup>12–14</sup>), both quadrupole and high-resolution magnetic sector inductively coupled plasma mass spectrometry (Q- and SF-ICP-MS;<sup>15–17</sup>), multi-collector inductively coupled plasma mass spectrometry (MC-ICP-MS;<sup>18–22</sup>), and secondary ionization mass spectrometry (SIMS;<sup>23–25</sup>) commonly used amongst the different fields. The choice of instrument depends on the application, but the highest precision (*i.e.*, best reproducibility) isotopic analyses are typically achieved on the MC-ICP-MS instruments.

Lithium isotopic compositions can be analyzed in either purified or unpurified samples, largely depending on the type of material being analyzed and the precision required for meaningful interpretation of results. Studies that determine lithium isotopic compositions in liquid samples or dissolved solids generally require purification,<sup>16,26</sup> and those that do not require careful consideration of matrix effects associated with *in situ* analyses in solids (*e.g.*, ref. 23, 27 and 28). Purification typically employs the use of cation exchange resin<sup>29</sup> that allows for

effective separation of Li from Na, which is often the most problematic element due to the difficulty of separation and associated matrix effects during analysis. Methodologies have included single and dual-column separations using AG50W-X8, AG50W-X12, and AG MP-50 resins, and different acids (hydrochloric and nitric) and mixtures of acids (hydrochloric and nitric) and methanol. A review of these procedures is provided in ref. 29. Regardless of the procedure being used, quantitative recovery of lithium is critical due to the potential for isotopic fractionation from the purification procedure.<sup>30</sup>

In this work, we demonstrate the use of the new Neoma MS/MS MC-ICP-MS to measure lithium isotopic compositions in several environmental and geological reference materials, including soils, sediments, rocks, and seawater. The Neoma MS/MS contains a novel pre-cell mass filter system, the double Wien filter, that directs the ion beam with magnetic and electrostatic fields. The light mass of lithium with only two isotopes makes tuning of this system critical, as it is can be relatively easy to clip or distort either the  ${}^6\text{Li}$  or  ${}^7\text{Li}$  beams and produce inaccurate and unstable isotope ratios. While there may not exist any particular advantage to using the MS/MS version of the Neoma for Li isotope analysis, the intention of this work is to demonstrate that the Neoma MS/MS is capable of producing Li isotopic data comparable to other MC-ICP-MS instruments that do not have mass filtering or collision cell capabilities. Additionally, a new chemical purification method that minimizes the amount of resin and the timeline for purification was

Pacific Northwest National Laboratory, Richland, Washington, USA. E-mail: sean.scott@pnnl.gov



presented. Despite the increased challenges associated with the double Wien prefilter system equipped on the Neoma MS/MS, lithium isotopes can be measured with similar accuracy and precision to standard MC-ICP-MS instruments (*i.e.*, those without collision cells or pre-filters). Using the Neoma MS/MS MC-ICP-MS and new methods proposed in this paper, we report the first lithium isotopic composition data for several widely-used NIST environmental standards.

## 2. Experimental

Mass spectrometry analyses were conducted on the Neoma™ MS/MS MC-ICP-MS (Thermo Scientific) at the Physical Sciences Facilities at Pacific Northwest National Laboratory. The Neoma MS/MS is equipped with 10 moveable Faraday cups, a fixed center Faraday cup, a center SEM/RPQ, and a nuclear package containing three fixed SEMs, two moveable CDDs, and a fixed Faraday cup located in the same position as SEM2. Several different reference materials were digested and analyzed for lithium isotopic composition, including NIST688, NIST1646a, NIST2706, NIST2709a, NIST2711a, NIST 2780a, NIST4350b, as well as USGS rock reference materials BCR-2, BHVO-2, BIR-1a, GSP-2, RGM-2, and W-2a. A pure lithium carbonate (NIST924a) was also digested and passed through the purification procedure during initial testing to demonstrate recoveries and lack of isotopic fractionation from the procedure. The primary reference material used for mass spectrometry analysis was LSVEC, a lithium carbonate with certified Li isotopic composition.<sup>31</sup>

### 2.1 Sample digestions

An aliquot of  $\sim$ 100 mg of NIST924a was transferred to a clean PFA bottle, and 18.2 M $\Omega$  H<sub>2</sub>O was added to reduce static. Optima grade HCl was then added slowly until the sample aliquot was completely dissolved (based on visual inspection). Additional HCl was added to produce a 2 M HCl solution containing  $\sim$ 600  $\mu$ g g<sup>-1</sup> Li.

Aliquots of the various SRM standards and USGS rocks analyzed by the Neoma MS/MS first underwent a complete dissolution which used various Optima Grade concentrated mineral acids, included nitric acid (HNO<sub>3</sub>), hydrochloric acid (HCl), hydrofluoric acid (HF), and perchloric acid (HClO<sub>4</sub>). For each sample or batch of samples undergoing dissolution, a dissolution blank was also used as a representative background measurement for each dissolution. Upon completion of the dissolution process, the samples were brought up in 2 M HCl with a concentration of  $\sim$ 10 mg soil per g solution. The detailed steps and volumes of reagents used varied depending on the amount and matrix of the material. A detailed example of a complete dissolution was provided in ref. 32 for NIST SRM2780a.

### 2.2 Lithium purification

Prior to analysis on the Neoma MS/MS, lithium was purified using an AG MP-50 (100–200 mesh) cation exchange procedure adapted from ref. 22 and 33. Testing of the purification

procedure was accomplished using rock reference materials, seawater, and NIST924a to determine the elution profile of lithium and other elements. Elution profiles were measured on a ThermoScientific iCAP TQ triple quadrupole inductively coupled plasma mass spectrometer. Approximately 1.5 ml of AG MP-50 resin were loaded into a column made from a pipette tip with a length of 12 cm and inner diameter of 4 mm. Once the resin was settled into the column, washes of 6 M HCl to clean the resin caused the resin to settle by  $\sim$ 1 cm. After cleaning the resin with 6 M HCl, the column is conditioned with 0.2 M HCl. Sample volumes of 125  $\mu$ l are loaded onto the column, and both 2 M HCl or seawater can be loaded directly. The matrix is eluted with 3 ml of 0.2 M HCl + 0.3 M HF, then 1.5 ml of 0.6 M HCl. The Li is then collected with 3 ml of 0.6 M HCl. The lithium fraction is dried, re-dissolved in 60  $\mu$ L of 16 M HNO<sub>3</sub>, and diluted to 2 ml with H<sub>2</sub>O. In general, the total Li quantities extracted from the chemistry were  $<$ 100 ng.

### 2.3 Tuning of the MS/MS

The pre-cell mass filter system on the Neoma MS/MS must be tuned to provide maximum transmission through the mass spectrometer.<sup>34</sup> Sensitivity is maximized by directing the ion beam through the center of the filter system. This is achieved by coupling of the B field and E field, such that increasing the B field requires an increase in the E field to maintain the ion velocity selection through the center of the filter system. Likewise, the B field can be reduced to decrease spread of the ions through the double Wien filter and should be set relatively low (for this work 5% of the maximum). A B field of 5% was chosen because this reduced the impacts of small variations (0.5 to 1 V) of the lenses of the Wien filter and of the E field on the measured isotopic ratio. Due to the susceptibility of the system to produce inaccurate and unstable lithium isotope ratios, the sensitivity should be tuned while simultaneously monitoring the isotope ratio, which was the approach used in this study. Additionally, the isotope ratio should be monitored when tuning the prefilter lenses as they can also impart a significant effect on the isotope ratio. In general, mass bias of lithium from sample introduction into the mass spectrometer is expected to be large. For example, the lithium isotope ratio in this study was tuned to <sup>6</sup>Li/<sup>7</sup>Li of  $\sim$ 0.066 (*vs.* a true ratio of 0.08215 for LSVEC<sup>31</sup>), which yielded a mass bias factor of  $\sim$ 23% while maintaining reproducible results.

While both the sensitivity and isotope ratio can appear adequate for isotopic analysis, the stability of the isotope ratio (*i.e.*, the standard deviation over the course of an analysis) might not meet normal expectations. Very small variations in the voltages (0.5 to 1 V) of the pre-filter lenses can impact the isotope ratio stability of an individual analysis. Before running any sample sequence, the tuning window is set to produce 4 seconds integrations, and 30 cycles are collected. Tuning is considered sufficient when the standard deviation of the 30 cycles is  $<$ 0.000025 on a <sup>6</sup>Li/<sup>7</sup>Li ratio of  $\sim$ 0.066 (or  $<$ 0.04%). Under optimal conditions the standard deviation approaches 0.000010.

In addition to tuning of the pre-filter lenses, the ion beam must also pass through the collision cell regardless of whether



any gas is used. Thus, the lenses and other settings (RF frequency and bias voltage) must also be optimized. The RF frequency was turned down to 20–25% of the maximum to allow Li to pass through the hexapole as recommended by the manufacturer. No gas was used in the collision cell. Typically, gases are employed to reduce and/or eliminate isobaric interferences. We observed no interferences on the isotopes of lithium that would require the use of collisional or reactive gases. Like tuning the pre-filter lenses, the exit and entry lenses of the cell were tuned to optimize sensitivity and isotopic ratio stability.

#### 2.4 Acquisition parameters

Purified solutions were diluted to provide 6 ppb of Li in 3%  $\text{HNO}_3$ , or in some cases analyzed without dilution when sample sizes were small. Samples were introduced into the plasma using an Elemental Scientific SC-microDX autosampler coupled to an ApexOmega desolvating nebulizer. The Jet sampler cone and “X” series skimmer cone were used to enhance sensitivity. The combination of the ApexOmega and Jet/X cones were required to measure the small sample sizes provided by the chemical purification. Like the MS/MS tuning, the ApexOmega gas flows are tuned to optimize sensitivity while maintaining stability in the measured isotopic ratio. Without the ApexOmega, high precision Li isotopic analyses using standard  $10^{11}$  Ohm resistors would not be possible based on the chemical purification scheme that provides <100 ng total Li.

Lithium isotopes were measured in static mode using the L5 and H5 Faraday cups to measure  $^6\text{Li}$  and  $^7\text{Li}$ , respectively. For samples with nominally natural isotope abundances,  $10^{11}$  Ohm resistors are used for both isotopes. Sample-standard bracketing was used to correct for mass bias with LSVEC ( $^6\text{Li}/^7\text{Li} = 0.08215 \pm 0.00023$ <sup>31</sup>) as the primary bracketing standard. On-peak baselines are measured before and after every sample and standard. Thus, each sample analysis contains a sequence of blank-standard-blank-sample-blank-standard-blank. All blanks, standards, and samples are measured for 30 cycles of 4 seconds integrations. Standards NIST924a, IRMM-016, and LSVEC (measured relative to itself) were measured over time to determine long-term reproducibility. Recoveries were calculated by comparing the Li concentration of the samples to the concentration of the known LSVEC standard. Blanks were estimated using the same method.

Data reduction occurs primarily in the Qtegra software, including on-peak blank corrections and calculation of average isotopic ratios and in-run statistics. The blank-corrected average isotopic ratios are exported from the Qtegra software, and mass bias is corrected using the average measured LSVEC value before and after each sample analysis. A linear correction is used as follows:

$$^6\text{Li}/^7\text{Li}_t = \frac{^6\text{Li}/^7\text{Li}_{r\text{-sample}}}{^6\text{Li}/^7\text{Li}_{r\text{-LSVEC}}} \times ^6\text{Li}/^7\text{Li}_{t\text{-LSVEC}} \quad (1)$$

Subscripts t and r refer to the true and raw isotopic ratios, respectively.

## 3. Results

Lithium isotope results for the standards measured in this study are provided in Table 1, and lithium isotopic compositions of the NIST924a aliquots passed through the chemical separation are provided in Table 2. Both the  $\delta^7\text{Li}$  and  $^6\text{Li}/^7\text{Li}$  values are reported, as well as the expected and measured total amount of Li from the separation procedure. For comparisons to literature values, the  $\delta^7\text{L}$  is used because this is a common way to report Li isotopic composition data:

$$\delta^7\text{Li} = \left( \frac{^7\text{Li}/^6\text{Li}_{\text{sample}}}{^7\text{Li}/^6\text{Li}_{\text{LSVEC}}} - 1 \right) \times 10^3 \quad (2)$$

$\delta^7\text{Li}$  agree well with the available literature data (Fig. 1), except for NIST688 with one analysis that has higher reported  $\delta^7\text{Li}$  than what was measured in this study ( $\delta^7\text{Li}$  of 2.9 (ref. 35) vs. 1.02 measured here). Aside from seawater with slightly depleted ( $^6\text{Li}$ ) isotope compositions, most materials show a relatively narrow range in isotopic composition generally near the nominally natural isotopic compositions represented by LSVEC, IRMM-016, and NIST924a. As of the time of publication, the long-term average of NIST924a was  $0.082268 \pm 0.000051$  ( $2\sigma, n = 152$ ), the long-term average of IRMM-016 was  $0.082148 \pm 0.000046$  ( $2\sigma, n = 105$ ), and the long-term average of LSVEC was  $0.082152 \pm 0.000042$  ( $2\sigma, n = 58$ ), starting in April 2023 (data for LSVEC provided in Fig. 2). The NIST924a aliquots purified through the AGMP-50 procedure gave  $^6\text{Li}/^7\text{Li} = 0.082248 \pm 0.000026$  ( $2\sigma, n = 7$ ; Table 2). NIST924a contains nominally natural isotopic compositions with  $^6\text{Li}/^7\text{Li} = 0.08223 \pm 0.00013$ .<sup>36</sup>

In general, recoveries for all samples were within a 10 percent of 100%, except for NIST688 with recoveries of ~135% assuming the concentration value reported in ref. 35 ( $4.9 \mu\text{g g}^{-1}$ ). New concentration measurements of this material were accomplished by isotope dilution and gave a new value of  $5.76 \mu\text{g g}^{-1}$ , providing recoveries within 10% of 100% (Table 1). NIST SRM 4350b does not list a quantitative value for Li, only a maximum level; therefore, a separate aliquot of this solution was measured for concentration by Q-ICP-MS independently to determine recovery (measured at  $22.1 \pm 0.62 \mu\text{g g}^{-1}$ ). Blank measurements included digestion blanks that accompanied the sample digestions, as well as column blanks that only reflect the Li blank of the column procedure. Column blanks ranged from 2.0 to 12.9 ( $n = 5$ ) picograms, and total procedural blanks ranged from 3.2 to 11 ( $n = 7$ ) picograms of Li per 125  $\mu\text{L}$  aliquot of digest solution (Table 3). These blank levels are well below the typical amount of Li processed through the chemical procedure, with BIR-1a containing the lowest estimated quantity of Li (3.86 ng of Li per aliquot).

## 4. Discussion

### 4.1 Impacts of poor tuning on internal isotope ratio precision

Internal isotope ratio precision is strongly dependent on the tuning parameters of the double-Wien filter lenses and the collision/reaction cell. Fig. 2 shows the results of a pre-filter E field



**Table 1** Lithium isotope results for rock, sediment, and soil reference materials

Material	Sample	${}^6\text{Li/}{}^7\text{Li}$	$2\sigma$	$\delta^7\text{Li}$	$2\sigma$	$n^a$	$\text{Li}^b\text{ (}\mu\text{g g}^{-1}\text{)}$	Expected (ng)	Measured <sup>d</sup> (ng)	Recovery
Basalt rock	NIST688_1 <sup>c</sup>	0.08220	0.00026	-0.66	3.16	3	5.8 (0.1)	7.7	8.3 (0.3)	107%
	NIST688_2	0.082082	0.000028	0.82	0.34	3	5.8 (0.1)	7.7	8.4 (0.2)	108%
	NIST688_3	0.082071	0.000058	0.96	0.71	3	5.8 (0.1)	7.7	8.1 (0.3)	105%
	NIST688_4	0.082070	0.000023	0.97	0.28	3	5.8 (0.1)	7.7	8.3 (0.1)	107%
	NIST688_5	0.082053	0.000037	1.19	0.46	3	5.8 (0.1)	7.7	8.1 (0.1)	105%
	NIST688_6	0.082050	0.000035	1.22	0.43	3	5.8 (0.1)	7.7	8.4 (0.1)	108%
Estuarine sediment	NIST1646a_1	0.081840	0.000051	3.79	0.63	3	18	11.1	11 (0.4)	100%
	NIST1646a_2	0.081878	0.000010	3.33	0.12	3	18	11.1	11 (0.1)	99%
New Jersey soil	NIST2706_1	0.081945	0.000043	2.50	0.53	3	16.4 (1.8)	20.6	20 (0.9)	99%
	NIST2706_2	0.081997	0.000008	1.86	0.10	3	16.4 (1.8)	20.6	20 (0.5)	97%
San Joaquin soil	NIST2709a_1	0.082215	0.000049	-0.80	0.59	3	51.9 (0.7)	62.9	61 (0.8)	97%
	NIST2709a_2	0.082156	0.000067	-0.08	0.82	3	51.9 (0.7)	62.9	59 (2.2)	94%
Montana II soil	NIST2709a_3	0.082157	0.000039	-0.08	0.47	3	51.9 (0.7)	62.9	60 (2.4)	96%
	NIST2711a_1	0.082173	0.000019	-0.28	0.23	3	29.1 (1.5)	35.4	39 (0.5)	110%
Hard rock mine waste	NIST2711a_2	0.082182	0.000022	-0.39	0.27	3	29.1 (1.5)	35.4	38 (0.6)	107%
	NIST2780a_1	0.081733	0.000013	5.10	0.15	3	14	8.5	8.8 (0.2)	103%
Columbia River sediment	NIST2780a_2	0.081810	0.000029	4.16	0.36	3	14	8.5	8.7 (0.4)	102%
	NIST4350b_1	0.082073	0.000005	0.94	0.06	3	22.1 (0.6)	27.3	30 (0.1)	109%
Hawaiian basalt	NIST4350b_2	0.082113	0.000046	0.45	0.56	3	22.1 (0.6)	27.3	30 (0.4)	111%
	NIST4350b_3	0.082059	0.000013	1.11	0.16	3	22.1 (0.6)	27.3	30 (0.02)	108%
Icelandic basalt	NIST4350b_4	0.082120	0.000018	0.37	0.22	3	22.1 (0.6)	27.3	30 (0.03)	109%
	NIST4350b_5	0.082079	0.000062	0.87	0.75	1	22.1 (0.6)	27.3	31 (0.1)	115%
Silver plume granodiorite	NIST4350b_6	0.082075	0.000019	0.92	0.23	3	22.1 (0.6)	27.3	27 (0.1)	99%
	NIST4350b_7	0.082152	0.000036	-0.02	0.44	3	22.1 (0.6)	27.3	27 (0.7)	99%
Glass Mountain rhyolite Database	Avg:	0.082096	0.000067	0.63	0.87	3	22.1 (0.6)	27.3		
	W-2a	0.081887	0.000021	3.22	0.25	3	9.13 (0.22)	11.02	11 (0.3)	103%
Carolina Seawater	BHR-2	0.081811	0.000025	4.14	0.31	3	4.50 (0.085)	5.46	5.8 (0.1)	106%
	BIR-1a	0.081875	0.000010	3.36	0.12	3	3.20 (0.069)	3.86	4.0 (0.01)	102%
Diabase	GSP-2	0.082141	0.000003	0.10	0.04	3	36 (ref. 1)	43.52	43 (0.1)	100%
	RGM-2	0.081977	0.000008	2.10	0.10	3	58 (ref. 2)	70.04	73 (0.1)	105%
Seawater	W-2a	0.081973	0.000006	2.16	0.07	3	9.21 (0.19)	11.14	11 (0.15)	102%
	Carolina Seawater_1	0.079687	0.000046	30.90	0.60	4	0.20	25	26 (0.1)	104%
Carolina Seawater	Carolina Seawater_2	0.079763	0.000010	29.93	0.13	4	0.20	25	24 (0.5)	98%
	Carolina Seawater_3	0.079740	0.000013	30.22	0.17	4	0.20	25	25 (0.1)	98%
Carolina Seawater	Carolina Seawater_4	0.079713	0.000044	30.57	0.57	4	0.20	25	25 (0.1)	100%
	Carolina Seawater_5	0.079674	0.000007	31.07	0.09	3	0.20	25	21 (0.1)	86%
Carolina Seawater	Carolina Seawater_6	0.079720	0.000014	30.49	0.35	3	0.20	25	22 (0.5)	88%
	Avg:	0.079716	0.000066	30.53	0.94					

<sup>a</sup> For samples with  $n = 1, 2$ , st. dev. internal precision is used. <sup>b</sup> Li concentrations are from the certificates (NIST1646a, NIST2706, NIST2780a, BCR-2, BHVO-2, BIR-1a, GSP-2, W-2a), average from GEOREM (RGM-2),<sup>40</sup> (NIST2709a and NIST2711a), or measured by ICP-MS (NIST4350b) or ID-MC-ICP-MS (NIST688) at PNNL. Parentheses indicate uncertainties as available. A nominal concentration of 0.2 ppm was assumed for seawater. <sup>c</sup> Value excluded in average shown in Fig. 1 due to high uncertainty. <sup>d</sup> Parentheses indicate uncertainties based on the standard deviation of concentrations measured in replicates and do not include other sources of uncertainties such as the standard used for intensity calibration.

**Table 2** Lithium isotope results of NIST924a aliquots passed through the AGMP50 resin

Aliquot	${}^6\text{Li}/{}^7\text{Li}$	$2\sigma$	Recovery
1S	0.082247	0.000039	101%
2S	0.082249	0.000004	102%
3S	0.082256	0.000047	103%
1G	0.082238	0.000032	102%
2G	0.082266	0.000027	104%
3G	0.082225	0.000036	101%
4G	0.082256	0.000025	102%
Average	0.082248	0.000027	

scan, which depicts small (0.5 V) incremental changes of the E field of the double Wien filters. The critical aspect of this tuning parameter is the offset in E field voltage between the maximum sensitivity and the small “plateau” of isotopic ratio stability over only a few V. As the  ${}^7\text{Li}$  beam intensity reaches a maximum, small (0.5 V) changes in the E field still produce relatively large changes in the  ${}^6\text{Li}/{}^7\text{Li}$  ratio (>0.2% per 0.5 V change on average). Increasing the E field from the maximum sensitivity point causes a minor decrease in sensitivity, until a point is reached where 0.5 V interval changes in the E field produce a minimum change in the  ${}^6\text{Li}/{}^7\text{Li}$  (<0.1% per 0.5 V on average). Beyond this “plateau” of isotope ratio stability, further increases in the E field result in drastic decreases in sensitivity (over an order of magnitude) and changes to the  ${}^6\text{Li}/{}^7\text{Li}$  far outside the value expected if only mass bias is acting on the measured isotope ratio.

Measurements of the LSVEC standard (bracketed relative to itself) show that even when tuning for maximum sensitivity and ion beam stability (*i.e.*, the RSD of individual beam intensities), internal precision is not always consistent (Fig. 3). The techniques required for tuning were determined over the course of this study by observing relatively large internal measurement precisions that exceeded what is normally expected on a multi-collector instrument using Faraday cups. In particular, the standard deviations of individual measurements can approach 0.000075 when the instrument is not

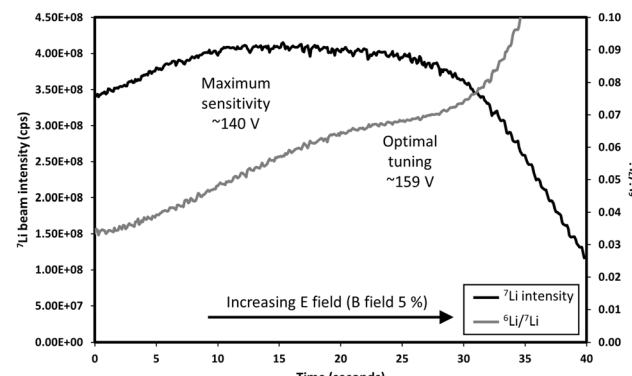


**Fig. 2** Diagram showing the  ${}^7\text{Li}$  beam intensity and  ${}^6\text{Li}/{}^7\text{Li}$  ratio as a function of time during an E field scan on the Neoma MS/MS. The window shows an E field scan beginning at  $\sim 135$  V and ending at  $\sim 180$  V. When maximum sensitivity is achieved, the isotopic ratio is still susceptible to instability due to the sensitivity of the ratio to the E field voltage. A “plateau” of isotope ratio stability is shown that is near the high voltage “shoulder” of the sensitivity plateau. Optimal tuning requires tuning of the isotope ratio stability, while minimally sacrificing sensitivity, as is the case for Li in this work.

**Table 3** Blank levels

Sample	Total Li (ng)
Digestion + column blank 1	0.0086
Digestion + column blank 2	0.0032
Digestion + column blank 3	0.0085
Digestion + column blank 4	0.0058
Digestion + column blank 5	0.0041
Digestion + column blank 6	0.0051
Digestion + column blank 7	0.0112
Column blank 1	0.0056
Column blank 2	0.0020
Column blank 3	0.0085
Column blank 4	0.0047
Column blank 5	0.0129

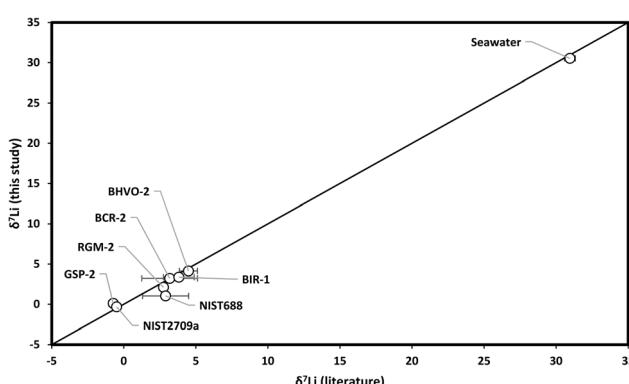


**Fig. 1** Comparison between average values measured in this study and literature values (error bars are 1 sigma). Data and sources for literature values are provided in the supplementary material, and include averages from GEOREM for BCR-2, BHVO-2, BIR-1, GSP-2, and Seawater (IAPSO). Values for RGM-2 are from ref. 38. Values for NIST688 are from ref. 35. Values for NIST2709a are from ref. 39.

tuned to minimize uncertainty in the isotopic ratio precision as was described in Section 2.3 and shown in Fig. 2. This effect can be attributed to the asymmetric mass transfer window of the double Wien filter shown in ref. 37, who noted the necessity for careful tuning of the pre-filter lenses to avoid clipping ion beam signals which could lead to instrument instability and isotopic fractionation. Despite these challenges, which are most apparent with lithium, comparison of data measured on the Neoma MS/MS to literature values (when available; Fig. 1) show that this instrument can be used to reproducibly measure high precision Li isotope ratios.

#### 4.2 Lithium isotope ratios of reference materials

Aside from the geological samples measured in this study, the various NIST soils and sediments contain very little variation in lithium isotopic abundances. The highest  $\delta^7\text{Li}$  (aside from



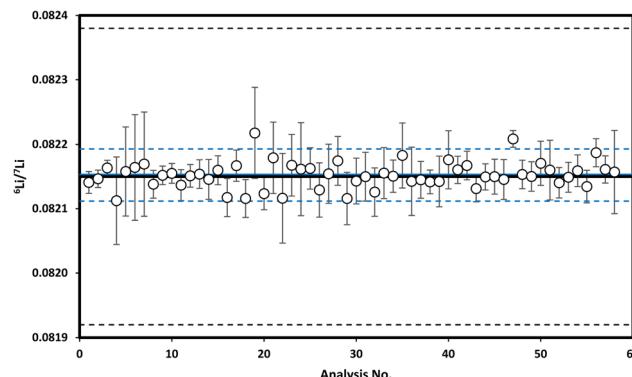


**Fig. 3** Lithium isotopic composition of LSVEC measured relative to itself during the duration of this study (~1.5 years). Large differences in internal precision (shown as 1SD) reflect variations in tuning parameters that cause instabilities in the measured isotope ratios during a single analysis. The effects of this tuning uncertainty were especially significant early on and was subsequently the focus of many analytical sessions. The solid black and dashed lines show the certified value for LSVEC ( $0.08215 \pm 0.00023$ ;<sup>31</sup>). The blue dashed lines show the 2-sigma interval of all analyses for this study, with the average (solid blue line) directly underneath the solid black line.

seawater) was measured in NIST2780a, although this value is still near the “natural” lithium isotope abundances. Despite the various sources of these materials and potential for fractionation by several geologic processes, these materials can provide a good baseline for analysis of different types of matrix materials with nominally natural isotopic abundances.

#### 4.3 Benefits of the single column AG MP-50 procedure

The chemistry procedure used in this study is advantageous in several ways. All the solutions loaded onto the column were taken directly from digested samples or seawater requiring no transposition of primary digested solutions (in 2 M HCl) or seawater. Only 125 µl of solution was loaded regardless of the matrix. This aspect makes the overall process quicker, requiring less than 8 hours for the purification, and does not use nitric acid-methanol mixtures, which present additional hazards compared to only acidic solutions (e.g., hydrochloric acid). Eliminating pre-column transpositions reduces one potential source of sample contamination during processing, and the blank levels were consistently low from the chemical procedure (maximum 13 pg). However, the total amount of Li is generally relatively small (<100 ng), which then requires the ApexOmega for the isotopic analysis. Overall, a single column procedure using the AG MP-50 resin is adequate for Li isotope separations and analysis when systems to improve instrumental sensitivity are used.

## 5. Conclusions

This work demonstrates the ability of the Neoma MS/MS to measure Li isotopic ratios in a variety of reference materials purified using AG MP-50 cation exchange resin. Isotopic compositions of reference materials are comparable to results from the literature, and those without literature values contain nominally

natural lithium isotope abundances. Despite the added difficulty of focusing the ion beam through the pre-cell double Wien Filter and collision/reaction cell, careful tuning of the lenses and other parameters of these systems can result in high precision lithium isotope ratio data.

## Data availability

The data supporting this article are included in the manuscript.

## Conflicts of interest

There are no conflicts of interest to declare.

## Acknowledgements

This work was sponsored by the Office of the Deputy Assistant Secretary of Defense for Nuclear Matters, as well as the Gateway for Accelerated Innovation in Nuclear administered by Idaho National Laboratory. Pacific Northwest National Laboratory is a multi-program national laboratory operated for the U.S. Department of Energy (DOE) by Battelle Memorial Institute under contract number DE-AC05-76RL01830. Matt Coble is acknowledged for internal review of the manuscript and two anonymous reviewers provided feedback that significantly improved the quality of the manuscript.

## References

- 1 L. H. Chan, J. M. Edmond, G. Thompson and K. Gillis, Lithium isotopic composition of submarine basalts: implications for the lithium cycle in the oceans, *Earth Planet. Sci. Lett.*, 1992, **108**, 151–160.
- 2 L. H. Chan, W. P. Leeman and T. Plank, Lithium isotopic composition of marine sediments, *Geochem., Geophys., Geosyst.*, 2006, **7**, Q06005.
- 3 J. S. Pistiner and G. M. Henderson, Lithium isotope fractionation during continental weathering processes, *Earth Planet. Sci. Lett.*, 2003, **214**, 327–339.
- 4 R. Halama, W. F. McDonough, R. L. Rudnick and K. Bell, Tracking the lithium isotopic evolution of the mantle using carbonatites, *Earth Planet. Sci. Lett.*, 2008, **265**, 726–742.
- 5 F. Z. Teng, R. L. Rudnick, W. F. McDonough, S. Gao, P. B. Tomascak and Y. Liu, Lithium isotopic composition and concentration of the deep continental crust, *Chem. Geol.*, 2008, **255**, 47–59.
- 6 J. G. Murphy, A. S. C. Ahm, P. K. Swart and J. A. Higgins, Reconstructing the lithium isotopic composition ( $\delta^7\text{Li}$ ) of seawater from shallow marine carbonate sediments, *Geochim. Cosmochim. Acta*, 2022, **337**, 140–154.
- 7 B. Kalderon-Asael, J. A. R. Katchinoff, N. J. Planavsky, AvS. Hood, M. Dellinger, E. J. Bellefroid, *et al.*, A lithium-isotope perspective on the evolution of carbon and silicon cycles, *Nature*, 2021, **595**, 394–398.
- 8 A. M. Desaulty, D. M. Climent, G. Lefebvre, A. Cristiano-Tassi, S. Perret, A. Urban, *et al.*, Tracing the origin of



lithium in Li-ion batteries using lithium isotopes, *Nat. Commun.*, 2022, **13**, 4172.

9 F. Carotti, B. Goh, M. Shafer and R. O. Scarlat, Datasets for elemental composition of 2LiFe-BeF<sub>2</sub> (FLiBe) salt purified by hydro-fluorination, analyzed by inductively coupled plasma mass spectrometry (ICP-MS) using two digestion methods, *Data Brief*, 2018, **10**, 1612–1617.

10 S. R. Scott and M. M. Shafer, A new method for measurement of lithium isotopes with nuclear applications, *Prog. Nucl. Energy*, 2020, **120**, 1–7.

11 S. R. Scott, F. Carotti, A. Kruizinga, R. O. Scarlat, S. Mastromarino and M. M. Shafer, Simultaneous measurement of lithium isotope and lithium/beryllium ratios in FLiBe salts using MC-ICP-MS, *J. Anal. At. Spectrom.*, 2022, **37**, 1193–1202.

12 L. H. Chan, Lithium isotope analysis by Thermal Ionization Mass Spectrometry of Lithium Tetraborate, *Anal. Chem.*, 1987, **59**, 2662–2665.

13 T. Moriguti and E. Nakamura, Precise Lithium Isotopic Analysis by Thermal Ionization Mass Spectrometry using Lithium Phosphate as an Ion Source Material, *Proc. Jpn. Acad. B: Phys. Biol. Sci.*, 1993, **69**, 123–128.

14 R. H. James and M. R. Palmer, The lithium isotope composition of international rock standards, *Chem. Geol.*, 2000, **166**, 319–326.

15 S. Misra and P. N. Froelich, Measurement of lithium isotope ratios by quadrupole-ICP-MS: application to seawater and natural carbonates, *J. Anal. At. Spectrom.*, 2009, **24**, 1524–1533.

16 X. M. Liu and W. Li, Optimization of lithium isotope analysis in geological materials by quadrupole ICP-MS, *J. Anal. At. Spectrom.*, 2019, **34**, 1708–1717.

17 M. S. Navarro, G. M. Paula-Santos, T. d. P. Marteleto and J. Enzweiler, Lithium isotopic ratios by single-collector ICP-SFMS: A critical evaluation using reference materials, *Geostand. Geoanal. Res.*, 2021, **45**, 701–718.

18 P. B. Tomascak, R. W. Carlson and S. B. Shirey, Accurate and precise determination of Li isotopic compositions by multi-collector sector ICP-MS, *Chem. Geol.*, 1999, **158**, 145–154.

19 R. Millot, C. Guerrot and N. Vigier, Accurate and high-precision measurement of lithium isotopes in two reference materials by MC-ICP-MS, *Geostand. Geoanal. Res.*, 2004, **28**, 153–159.

20 A. B. Jeffcoate, T. Elliott, A. Thomas and C. Bouman, Precise, small sample size determination of lithium isotopic compositions of geological reference materials and modern seawater by MC-ICP-MS, *Geostand. Geoanal. Res.*, 2004, **28**, 161–172.

21 M. Rosner, L. Ball, B. Peucker-Ehrenbrink, J. Blusztajn, W. Bach and J. Erzinger, A simplified, accurate and fast method for lithium isotope analysis of rocks and fluids, and  $\delta^{7Li}$  values of seawater and rock reference materials, *Geostand. Geoanal. Res.*, 2007, **31**(2), 77–88.

22 M. S. Bohlin, S. Misra, N. Lloyd, H. Elderfield and M. J. Bickle, High-precision determination of lithium and magnesium isotopes utilising single column separation and multi-collector inductively coupled plasma mass spectrometry, *Rapid Commun. Mass Spectrom.*, 2018, **32**, 93–104.

23 D. R. Bell, R. L. Hervig, P. R. Buseck and S. Aulbach, Lithium isotope analysis of olivine by SIMS: Calibration of a matrix effect and application to magmatic phenocrysts, *Chem. Geol.*, 2009, **258**, 5–16.

24 Z. Teichert, M. Bose and L. B. Williams, Lithium isotope compositions of U.S. coals and source rocks: Potential tracer of hydrocarbons, *Chem. Geol.*, 2020, **549**, 119694.

25 A. C. Denny, M. M. Zimmer, H. S. Cunningham and N. E. Sievers, Sources of Li isotope bias during SIMS analysis of standard glasses, *Chem. Geol.*, 2024, **656**, 122015.

26 W. Li, X. M. Liu and L. V. Godfrey, Optimisation of lithium chromatography for isotopic analysis in geological reference materials by MC-ICP-MS, *Geostand. Geoanal. Res.*, 2019, **43**, 261–276.

27 P. le Roux, Lithium isotope analysis of natural and synthetic glass by laser ablation MC-ICP-MS, *J. Anal. At. Spectrom.*, 2010, **25**, 1033–1038.

28 L. K. Steinmann, M. Oeser, I. Horn, H. M. Seitz and S. Weyer, In situ high-precision lithium isotope analyses at low concentration levels with femtosecond-LA-MC-ICP-MS, *J. Anal. At. Spectrom.*, 2019, **34**, 1447–1458.

29 X. Li, G. Han, Q. Zhang, R. Qu and Z. Miao, Accurate lithium isotopic analysis of twenty geological reference materials by multi-collector inductively coupled plasma mass spectrometry, *Spectrochim. Acta, Part B*, 2022, **188**, 106348.

30 L. F. Gou, C. Y. Liu, L. Deng and Z. Jin, Quantifying the impact of recovery during chromatographic purification on the accuracy of lithium isotopic determination by multi-collector inductively coupled plasma mass spectrometry, *Rapid Commun. Mass Spectrom.*, 2019, **34**, e8577.

31 H. P. Qi, P. D. P. Taylor, M. Berglund and P. De Bièvre, Calibrated measurements of the isotopic composition and atomic weight of the natural Li isotopic reference material IRMM-016, *Int. J. Mass Spectrom. Ion Processes*, 1997, **171**, 263–268.

32 S. R. Scott, K. P. Hobbs, A. D. French, I. J. Arnquist, S. Alcantar Anguiano, D. L. Sullivan, *et al.*, Uranium isotopic analysis in unpurified solutions by ICP-MS, *J. Anal. At. Spectrom.*, 2024, **39**, 2106–2115.

33 G. Zhu, J. Ma, G. Wei and L. Zhang, A rapid and simple method for lithium purification and isotopic analysis of geological reference materials by MC-ICP-MS, *Front. Chem.*, 2020, **2020**, 557489.

34 G. Craig, H. Wehrs, D. G. Bevan, M. Pfeifer, J. Lewis, C. D. Coath, *et al.*, Project Vienna: A novel precell mass filter for collision/reaction cell MC-ICPMS/MS, *Anal. Chem.*, 2021, **93**, 10519–10527.

35 H. M. Seitz, G. P. Brey, Y. Lahaye, S. Durali and S. Weyer, Lithium isotopic signatures of peridotite xenoliths and isotopic fractionation at high temperature between olivine and pyroxenes, *Chem. Geol.*, 2004, **212**, 163–177.

36 S. R. Scott, J. Williams, S. Mastromarino, N. Gajos, C. Berry, I. Anderson, *et al.*, Round-robin analysis of highly depleted lithium for Generation IV nuclear reactor applications, *Nucl. Eng. Des.*, 2024, **429**, 113664.



37 P. Telouk, E. Albalat, B. Bourdon, F. Albarede and V. Balter, Performance of the double-Wien filter of the Neoma MC-ICPMS/MS with an application to copper stable isotope compositions, *J. Anal. At. Spectrom.*, 2023, **38**, 1973–1983.

38 J. Lin, Y. Liu, Z. Hu, L. Yang, K. Chen, C. Haihong, *et al.*, Accurate determination of lithium isotope ratios by MC-ICP-MS without strict matrix-matching by using a novel washing method, *J. Anal. At. Spectrom.*, 2016, **31**, 390–397.

39 M. Weynell, U. Wiechert and J. A. Schuessler, Lithium isotopes and implications on chemical weathering in the catchment of Lake Dongji Cona, northeastern Tibetan Plateau, *Geochim. Cosmochim. Acta*, 2017, **213**, 155–177.

40 H. L. Byers, L. J. McHenry and T. J. Grundl, Forty-nine major and trace element concentrations measured in soil reference materials NIST SRM 2586, 2587, 2709a, 2710a, and 2711a using ICP-MS and wavelength dispersive-XRF, *Geostand. Geoanal. Res.*, 2016, **40**, 433–445.

